Cellular/Molecular

Deletion of *Vax1* from Gonadotropin-Releasing Hormone (GnRH) Neurons Abolishes GnRH Expression and Leads to Hypogonadism and Infertility

Hanne M. Hoffmann,[1] Crystal Trang,[1] Ping Gong,[1] Ikuo Kimura,[2] Erica C. Pandolfi,[1] and Pamela L. Mellon[1]

[1]Department of Reproductive Medicine and the Center for Reproductive Science and Medicine, University of California, San Diego, La Jolla, California 92093-0674, and [2]Department of Applied Biological Science, Graduate School of Agriculture, Tokyo University of Agriculture and Technology, Fuchu-shi 183-8509, Japan

Hypothalamic gonadotropin-releasing hormone (GnRH) neurons are at the apex of the hypothalamic-pituitary-gonadal axis that regulates mammalian fertility. Herein we demonstrate a critical role for the homeodomain transcription factor ventral anterior homeobox 1 (VAX1) in GnRH neuron maturation and show that *Vax1* deletion from GnRH neurons leads to complete infertility in males and females. Specifically, global *Vax1* knock-out embryos had normal numbers of GnRH neurons at 13 d of gestation, but no GnRH staining was detected by embryonic day 17. To identify the role of VAX1 specifically in GnRH neuron development, $Vax1^{flox}$ mice were generated and lineage tracing performed in $Vax1^{flox/flox}$:$GnRH^{cre}$:*RosaLacZ* mice. This identified VAX1 as essential for maintaining expression of *Gnrh1*. The absence of GnRH staining in adult $Vax1^{flox/flox}$:$GnRH^{cre}$ mice led to delayed puberty, hypogonadism, and infertility. To address the mechanism by which VAX1 maintains *Gnrh1* transcription, the capacity of VAX1 to regulate *Gnrh1* transcription was evaluated in the GnRH cell lines GN11 and GT1-7. As determined by luciferase and electrophoretic mobility shift assays, we found VAX1 to be a direct activator of the GnRH promoter through binding to four ATTA sites in the GnRH enhancer (E1) and proximal promoter (P), and able to compete with the homeoprotein SIX6 for occupation of the identified ATTA sites in the GnRH promoter. We conclude that VAX1 is expressed in GnRH neurons where it is required for GnRH neuron expression of GnRH and maintenance of fertility in mice.

Key words: fertility; GnRH; hypogonadism; transcription; ventral anterior homeobox

Significance Statement

Infertility classified as idiopathic hypogonadotropic hypogonadism (IHH) is characterized by delayed or absent sexual maturation and low sex steroid levels due to alterations in neuroendocrine control of the hypothalamic-pituitary-gonadal axis. The incidence of IHH is 1–10 cases per 100,000 births. Although extensive efforts have been invested in identifying genes giving rise to IHH, >50% of cases have unknown genetic origins. We recently showed that haploinsufficiency of ventral anterior homeobox 1 (*Vax1*) leads to subfertility, making it a candidate in polygenic IHH. In this study, we investigate the mechanism by which VAX1 controls fertility finding that VAX1 is required for maintenance of *Gnrh1* gene expression and deletion of *Vax1* from GnRH neurons leads to complete infertility.

Introduction

Sexual maturation is associated with increased activity of gonadotropin-releasing hormone (GnRH) neurons and the resultant pulsatile release of GnRH into the hypothalamic-hypophyseal portal system. Lack of GnRH secretion or absence of its receptor can lead to lack of or delayed puberty, and infertility

Received July 17, 2015; revised Jan. 5, 2015; accepted Feb. 1, 2016.

Author contributions: H.M.H., C.T., P.G., I.K., and P.L.M. designed research; H.M.H., C.T., P.G., I.K., and E.C.P. performed research; H.M.H., I.K., and P.L.M. contributed unpublished reagents/analytic tools; H.M.H., C.T., P.G., I.K., and P.L.M. analyzed data; H.M.H., C.T., P.G., and P.L.M. wrote the paper.

This work was supported by National Institutes of Health (NIH) Grants R01 DK044838, R01 HD072754, and R01 HD082567 (P.L.M.), the National Institute of Child Health and Human Development/NIH through a cooperative agreement (U54 HD012303) as part of the Specialized Cooperative Centers Program in Reproduction and Infertility Research (P.L.M.), partially supported by P30 DK063491, P30 CA023100, and P42 ES101337 (P.L.M.); The Kyoto University Foundation Fellowship Research Grant (I.K.); IMSD NIH Grant R25 GM083275 and a supplement to NIH R01 HD072754 (E.C.P.); and an Endocrine Society Summer Research Fellowship (C.T.). The University of Virginia, Center for Research in Reproduction, Ligand Assay, and Analysis Core is supported by the Eunice Kennedy Shriver NICHD/NIH (SCCPIR) Grant U54 HD28934. We thank Erica L. Schoeller and Genevieve E. Ryan for reading the paper, Shunichi Shimasaki for assistance with ovarian morphology interpretation, Erica L. Schoeller with testis morphology evaluation, and Brittainy M. Hereford with staining.

The authors declare no competing financial interests.

Correspondence should be addressed to Dr Pamela L. Mellon, University of California, San Diego, 9500 Gilman Drive, La Jolla, CA 92093-0674. E-mail: pmellon@ucsd.edu.

DOI:10.1523/JNEUROSCI.2723-15.2016

 0270-6474/16/363506-13$15.00/0

(Mason et al., 1986; Valdes-Socin et al., 2014). The origins of these conditions are mainly genetic and in some cases may be traced to alterations of GnRH neuron migration and maturation during embryonic development. Infertility classified as idiopathic hypogonadotropic hypogonadism (IHH) is characterized by delayed or absent sexual maturation, and low gonadotropin and sex steroid levels due to an alteration of the hypothalamic-pituitary-gonadal (HPG) axis (Bianco and Kaiser, 2009; Chan et al., 2009). Sixty percent of IHH cases present with anosmia, defective GnRH and olfactory neuron migration, and are classified as Kallmann syndrome (Dodé et al., 2006; Tsai and Gill, 2006; Pitteloud et al., 2007b). Despite great efforts, ~50% of IHH cases still have unknown genetic origins (Pitteloud et al., 2007a; Bianco and Kaiser, 2009).

In contrast to most CNS neurons, GnRH neurons originate in the olfactory placode at embryonic day (E)11 in the mouse, migrating through the cribriform plate, reaching their final location in the hypothalamus ~E16 (Schwanzel-Fukuda and Pfaff, 1989; Wierman et al., 2011). GnRH neuron migration and final localization is restricted to the ventral forebrain. Thus, homeodomain transcription factors expressed ventrally between E10 and E18 could be involved in the correct maturation and migration of GnRH neurons, making them candidate genes for IHH. This idea is supported by studies of full body and conditional knock-out mouse models in which the absence of specific homeobox genes affects GnRH neuron numbers and leads to various degrees of subfertility or complete infertility (Givens et al., 2005; Diaczok et al., 2011; Larder et al., 2011, 2013). Homeodomain proteins are characterized by preferential binding to ATTA sites in target gene promoters and play fundamental roles during embryogenesis. Ventral anterior homeobox 1 (VAX1) is a homeodomain protein required for ventral forebrain development, midline crossing, and eye formation (Hallonet et al., 1998, 1999; Take-uchi et al., 2003; Bharti et al., 2011). *Vax1* expression in adulthood is very sparse and is principally restricted to the ventral part of the hypothalamus (www.brain-map.org). *Vax1* knock-out (KO) mice die soon after birth due to cleft lip/palate, which prevents suckling. Due to the overlap in time and localization of *Vax1* and *Gnrh1* during embryogenesis, we hypothesized that VAX1 could be important for GnRH neuron development. Indeed we determined that heterozygosity of *Vax1* reduced the number of GnRH-expressing neurons by >50% in the adult brain (Hoffmann et al., 2014). This reduction in GnRH neuron numbers led to both male and female subfertility. Although *Vax1* heterozygote males had normal luteinizing hormone (LH), follicle-stimulating hormone (FSH), and testosterone levels, they presented with poor sperm quality, possibly due to an unidentified role of VAX1 in the testis. On the other hand, *Vax1* female heterozygosity led to higher circulating estrogen and LH in diestrus, which was associated with increased *Kiss1* in the anteroventral periventricular nucleus. This study identified *Vax1* as a potential candidate in polygenic IHH. Fertility maintenance requires only a handful of functional GnRH neurons (Herbison et al., 2008), it therefore remains unclear whether the subfertility of *Vax1* heterozygote mice is due to a combined role of VAX1 in GnRH neurons, as well as other brain areas and/or the testis. To determine the specific role of *Vax1* in GnRH neurons and its relation to IHH we generated $Vax1^{flox}$ mice and crossed them with $GnRH^{cre}$ mice allowing us to identify the specific role of VAX1 in GnRH neurons *in vivo*.

Materials and Methods

Cell culture. GT1-7 (Mellon et al., 1990), GN11 (kindly provided by Sally Radovick, Rutgers University, NJ), NIH3T3 (American Type Culture Collection), and COS-1 (American Type Culture Collection) cell lines were cultured in DMEM (Mediatech), containing, 10% fetal bovine serum (Gemini Bio), and 1× penicillin-streptomycin (Life Technologies/Invitrogen) in a humidified 5% CO_2 incubator at 37°C. For luciferase assays GT1-7 and GN11 cells were seeded into 24-well plates (Nunc) at 100,000 and 35,000 per well, respectively. Cells transfected for quantitative real-time PCR (qRT-PCR) were plated into 6-well plates (Nunc) at 400,000 (GT1-7) and 140,000 (GN11, NIH3T3) cells per well. Transfection of cells was done ~21–24 h after the cells were plated. Cells used for electrophoretic mobility shift assay (EMSA) and RNA sequencing were harvested at subconfluency 48–56 h after seeding in 10 cm dishes (Nunc).

qRT-PCR. Total RNA from GT1-7, GN11, and NIH3T3 cells was extracted using TRIzol (Invitrogen) according to the manufacturer's recommendations. DNA was eliminated by the use of DNA-free kit (Applied Biosystems), then cDNA was obtained by reverse transcription of RNA using iScript cDNA synthesis kit (Bio-Rad). cDNA products were detected using iQ SYBR Green Supermix (Bio-Rad) on a Q-RT PCR iQ5 real-time detection system (Bio-Rad). Primers to the coding sequences for mouse *Gnrh1* (F: TGCTGACTGTGTGTTTGGAAGGCT, R: TTTGATCCACCTCCTTGCGACTCA), *Vax1* (F: CCGGATCCTAGTCCGAGATGCC, R: TCTCCCGGCCCACCACGTAT), *Ppia* (F: AAGTTCCAAAGACAGCAGAAAAC, R: CTCAAATTTCTCTCCGTAGATGG), and *H2afz* (F: TCACCGCAGAGGTACTTGAG, R: GATGTGTGGGATGACACCA) permitted amplification of the indicated cDNA products. Data were expressed by the $2^{-\delta\delta CT}$ method by normalizing *Gnrh1* and *Vax1* to the housekeeping genes *Ppia* and *H2afz* (Livak and Schmittgen, 2001). Data are expressed as fold-change compared with control, or as indicated in the figure legends. Data represent mean fold-change ± SEM from a minimum of three independent RNA samples for each data point.

Transfection. Transient transfections for luciferase assays, qRT-PCR and EMSA were performed using PolyJet (SignaGen Laboratories) or Fugene HD (Roche Diagnostics), according to the manufacturer's recommendations. For luciferase assays, cells were cotransfected as indicated in the figure legends, with 150 ng/well luciferase reporter plasmids as previously described (Nelson et al., 2000; Iyer et al., 2010; Larder et al., 2011) and 100 ng/well thymidine kinase-β-galactosidase reporter plasmid as an internal control for transfection efficiency. Cells were cotransfected with expression vectors containing *Vax1* or *Vax1*-Flag in a CMV6 backbone (CMV; True Clone, Origene) or *Six6* in a pcDNA3.1 backbone (Larder et al., 2011). To equalize the amount of DNA transfected into cells, we systematically equalized plasmid concentrations by adding varying concentrations of the appropriate empty vector.

To specifically knock down *Vax1*, GT1-7 cells seeded in 6-well plates were transfected with 4 ng/well of Vax1 siRNA or scrambled siRNA (Santa Cruz Biotechnologies) using the siRNA reagent system (Santa Cruz Biotechnologies) following the manufacturer's instructions. Cells were harvested 32 h after the start of transfection.

Luciferase assay. Cells were harvested 21 h after transfection in lysis buffer(100 mM potassium phosphate, pH 7.8, and 0.2% Triton X-100). Luciferase and β-galactosidase assays were performed as previously described (Givens et al., 2005). Luciferase values are normalized to β-galactosidase values to control for transfection efficiency. Values are normalized to pGL3 or corresponding backbone of expression plasmid as indicated in the figure legends. Data represent the mean ± SEM of at least three independent experiments done in triplicate.

Cytoplasmic and nuclear extracts. COS-1 cells were scraped in hypotonic buffer (20 mM Tris-HCl, pH 7.4, 10 mM NaCl, 1 mM $MgCl_2$, 10 mM NaF, 1 mM phenylmethylsulfonyl fluoride, 1× protease inhibitor cocktail; Sigma-Aldrich)and left on ice to swell. Cells were lysed and nuclei were collected by centrifugation (4°C, 1700 × *g*, 4 min). Supernatant was collected and snap frozen until use for Western blot. Nuclear proteins were extracted on ice for 30 min in hypertonic buffer [20 mM HEPES, pH 7.9, 20% glycerol, 420 mM KCl, 2 mM $MgCl_2$, 10 mM NaF, 0.1 mM EDTA, 0.1 mM EGTA, 1× protease inhibitor cocktail (Sigma-Aldrich), and 1 mM phenylmethylsulfonylfluoride]. Debris was eliminated by centrifugation (4°C, 20,000 × *g*, 10 min), and supernatant was snap-frozen and stored

at −80°C until use. Protein concentration was determined using the Bio-Rad Protein Assay.

Western blotting. Cytoplasmic and nuclear proteins were dissolved and denatured in loading buffer. Ten micrograms of protein were separated by 12% SDS-PAGE. Proteins were transferred to a polyvinylidene fluoride membrane (Millipore), washed in PBS 0.05% Tween 20 (PBS-T), followed by blocking in 3% nonfat dry milk (Apex, Bioresearch Products, Genesee Scientific) dissolved in PBS-T. Primary antibodies were prepared in 1% milk dissolved in PBS-T and incubated overnight at 4°C with gentle agitation. Goat anti-mouse (1:1000; Santa Cruz Biotechnology, SC-2005) horseradish peroxidase (HRP)-conjugated secondary antibody was incubated at room temperature for 2 h. Antibody binding was detected by enhanced chemiluminescence (Thermoscientific). Immunoblotting was performed using primary antibodies against: mouse anti-DKK (Flag antibody, 1:3000; Origene, TA50011), mouse TATA-binding protein (TBP; 1:500; Abcam, AB818), and mouse GAPDH-HRP (1:2000; Abcam, 9482). Image visualization and preparation was performed using ImageJ (NIH Image).

Electrophoretic mobility shift assay. Oligonucleotide probes are listed in Figure 6*D*. All synthetic oligonucleotides were made by IDT. Annealed double-stranded oligonucleotides (1 pmol/μl) were end-labeled with T4 polynucleotide kinase (New England Biolabs) and [γ^{32}P]ATP (7000 Ci/mmol; MP Biomedicals). Probes were purified using Micro Bio-Spin 6 Chromatography Columns (Bio-Rad). Binding reactions contained 2 μg nuclear protein and 1 fmol of labeled probe in 10 mM HEPES, pH 7.9, 25 mM KCl, 2.5 mM MgCl2, 1% glycerol, 0.1% Nonidet P-40, 0.25 mM EDTA, 0.25% BSA, 1 mM dithiothreitol, and 350 ng poly(dI-dC). For competition experiments, 100-fold excess cold competitor probes were added. For supershift experiments, 2 μg of mouse anti-DKK (Flag antibody; Origene, TA50011) or 2 μg of normal mouse IgG (Santa Cruz Biotechnology, sc2025) were added to the reaction. Samples were incubated for 20 min at room temperature before loading on a 5% nondenaturing polyacrylamide gel in 0.25× Tris-borate EDTA buffer. Gels were run for 2 h at 200 V, dried under vacuum, and exposed to film for 2–5 d at room temperature.

Mouse breeding. All animal procedures were performed in accordance with the UCSD Institutional Animal Care and Use Committee regulations. Mice were group-housed on a 12 h light/dark cycle with *ad libitum* chow and water. *Vax1*^{tm1Grl} (Bertuzzi et al., 1999), here referred to as *Vax1* mice, were kindly provided by Dr Bharti (National Institutes of Health, Bethesda, MD). *Vax1*^{flox} mice were generated from the KO allele with conditional potential *Vax1*$^{tm1a(KOMP)Mbp}$ obtained from KOMP (UC Davis, Knock-Out Mouse Project, www.komp.org). *Vax1* knockout first mice (*Vax1*$^{tm1a(KOMP)Mbp}$ mice) were crossed with a *flpase* mouse (Rodríguez et al., 2000; http://jaxmice.jax.org/strain/003800.html) to generate a *Vax1* conditional KO allele, here referred to as *Vax1*^{flox} mice. *Vax1*^{flox} genotyping was performed with *Vax1*^{flox} forward: 5′GCCGGAACCGAAGTTCCTA 3′; *Vax1*^{wt} forward: 5′CCAGTAA GAGCCCCTTTGGG 3′, reverse 5′ CGGATAGACCCCTTGGCATC 3′. *Vax1*^{flox} mice were crossed with *GnRH*^{cre} (Wolfe et al., 2008) to generate *Vax1*^{flox}*:GnRH*^{cre} mice. For lineage tracing *Rosa-LacZ* (Soriano, 1999; http://jaxmice.jax.org/strain/003309.html) or *Rosa-YFP* (Srinivas et al., 2001) reporter mice were used. All mice were kept on a C57BL background. Mice were killed by CO_2 or isoflurane (Vet One, Meridian) overdose and decapitation.

Determination of pubertal onset and estrus cyclicity. These procedures were described previously in detail (Hoffmann et al., 2014). To assess estrous cyclicity, vaginal smears were performed daily between 9:00 and 11:00 A.M. on 3- to 5-month-old mice by vaginal lavage.

Timed mating. Each heterozygote female mouse was housed with a heterozygote male mouse, and vaginal plug formation was monitored. If a plug was present, the day was noted as day 0.5 of pregnancy and used to collect embryos for timed mating at E13.5, E15.5, and E17.5.

Fertility assessment. At 12–15 weeks of age, virgin *Vax1*^{flox} (control), *Vax1*$^{flox/+}$*:GnRH*^{cre} (cHET) and *Vax1*$^{flox/flox}$*:GnRH*^{cre} (cKO) mice were housed in pairs. The number of litters produced in 90 d was recorded.

Hormone levels and GnRH and Kisspeptin-10 challenges. Tail blood was collected from male and female metestrus/diestrus littermates. Ten minutes after receiving an intraperitoneal injection of 1 μg/kg GnRH in physiological serum, or 20 min after receiving an intraperitoneal injection of 3 mmol kisspeptin-10 in physiological serum, a second collection of tail blood was performed. The total volume of blood collected did not exceed 100 μl. Blood was allowed to clot for 1 h at room temperature, and then centrifuged (15 min, 2600 × *g*). Serum was collected and stored at −20°C before ELISA analysis of LH and FSH. Blood was collected between 9:00 A.M. and 12:00 P.M. Samples were run as singlet on MILIPLEX (#MPTMAG-49K, Millipore). LH: lower detection limit: 5.6 pg/ml, intra-ACOV 15.2, and inter-ACOV 4.7%. FSH: lower detection limit: 24.9 pg/ml, intra-ACOV 13.7, and inter-ACOV 3.9%. Estradiol was measured at the University of Virginia, Center for Research in Reproduction, Ligand Assay and Analysis Core. Lower detection limit: 3.6 pg/ml, 6.1 intra-ACOV, and inter-ACOV 8.9%.

Embryo collection. Embryos were generated through timed-mating. For immunohistochemistry (IHC), embryos were fixed in 60% ethanol, 30% formaldehyde, and 10% acetic acid, overnight at 4°C, then dehydrated in 70% ethanol before paraffin embedding. Sagittal sections (10 μm) were cut on a microtome and floated onto SuperFrost Plus slides (Thermo Fisher Scientific).

Immunohistochemistry. IHC was performed as previously described (Hoffmann et al., 2014), with the only modification being antigen retrieval by boiling the samples for 10 min in 10 mM sodium citrate. Briefly, the primary antibody used was rabbit anti-GnRH (1:1000; Thermo Fisher Scientific, PA1-121) or rabbit anti-GnRH (1:1000; Novus, NBP2-22444). GnRH-positive neurons were counted throughout the brain. The nasal, cribriform plate, and hypothalamic regions were counted separately in the embryo, but the whole brain was counted for the adult. For lineage tracing, LacZ expression was detected with a chicken anti-LacZ primary antibody (1:1000; Abcam, ab9361) or yellow fluorescent protein (YFP) expression was detected with a rabbit-anti YFP primary antibody (1:500; Abcam, ab62341). Texas Red (Vector Laboratories) was used to counterstain sections as directed by the manufactures instructions.

Collection of uterus, ovary, testis, and gonadal histology. Ovaries and uteri from diestrus females and testes from males were dissected and weighed from animals of 2.8–4 months of age. Ovaries and testes were fixed for 1.5 h at room temperature and O/N at 4°C, respectively, in 60% ethanol, 30% formaldehyde, 10% glacial acetic acid. Gonads were paraffin embedded, serially sectioned at 10 μm, and stained with hematoxylin and eosin (H&E) (Sigma-Aldrich). Histology was examined, and the number of corpora lutea in the ovaries recorded and presence of sperm in the testis assessed.

Statistical analysis. Statistical analyses were performed using either Student's *t* test, one-way ANOVA or two-way ANOVA, followed by *post hoc* analysis by Tukey or Bonferroni as indicated in figure legends, with $p \leq 0.05$ to indicate significance.

Results

Correct GnRH neuron development requires VAX1 expression

Previously, we have shown that adult *Vax1* heterozygote (HET) mice had a >50% reduction of GnRH neurons leading to subfertility (Hoffmann et al., 2014). As *Vax1* is highly expressed in the anterior ventral forebrain between E8 and E18 (Hallonet et al., 1998, 1999), we hypothesized that absence of *Vax1* during development would be responsible for the reduction of GnRH neurons in the adult. To test this hypothesis, we collected *Vax1* wild-type (WT), HET, and KO embryos at E13.5 and E17.5, and counted the number of GnRH neurons by immunohistochemistry. At E13.5, GnRH neuron counts were comparable in *Vax1* WT, HET, and KO embryos (Fig. 1*A–D*), although a slight, yet statistically significant, decrease in the number of GnRH neurons at the cribriform plate (crib. plate) was found in the HET embryos (Fig. 1*B*,*C*). In contrast, at E17.5, *Vax1* KO embryos exhibited a complete loss of GnRH-expressing neurons in the brain (Fig. 1*E–H*). Counting GnRH neurons in the nasal placode area (nose), cribriform plate (crib. plate), and hypothalamic area (hypo, Fig. 1*G*) revealed that GnRH neurons were present at

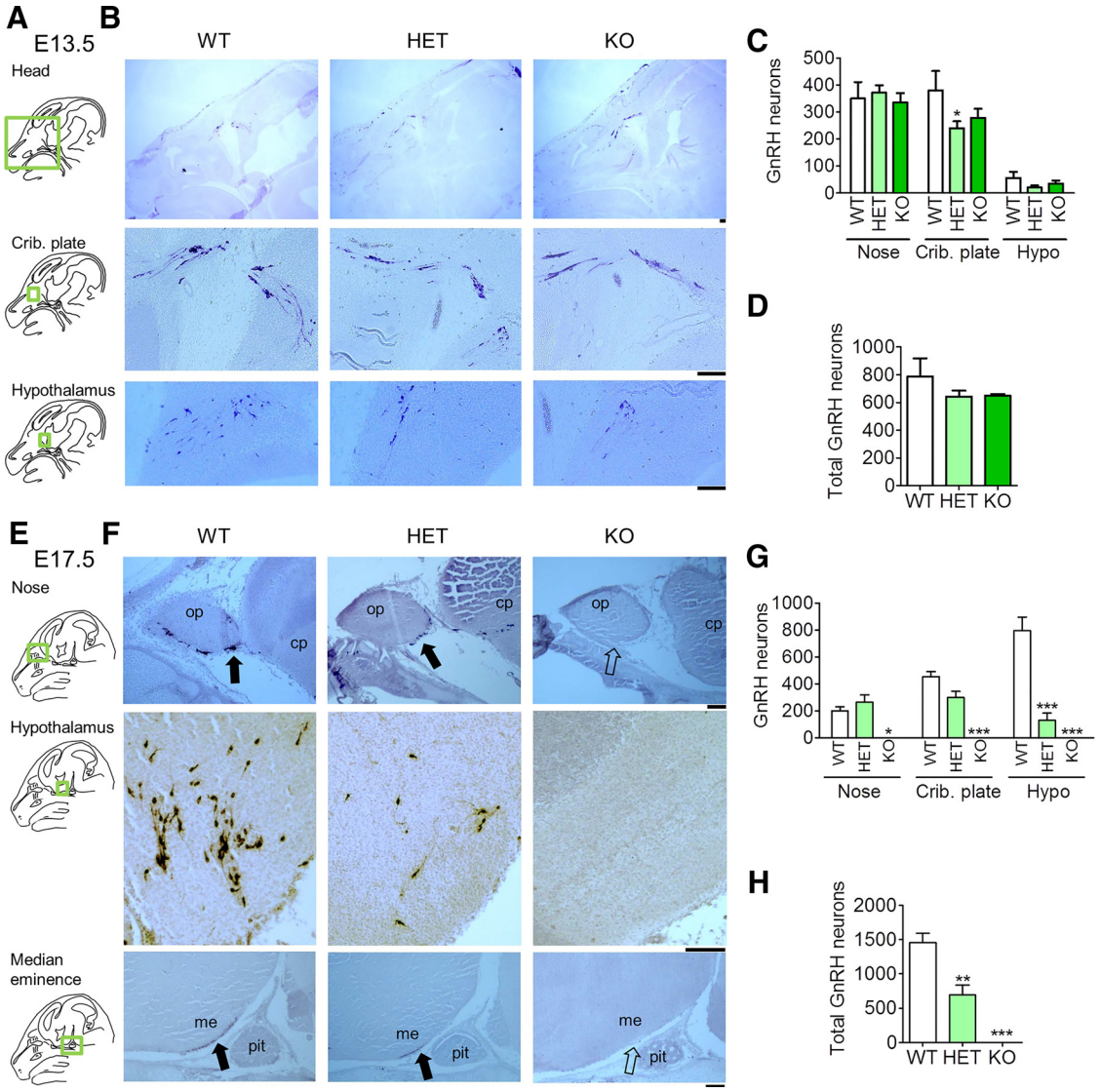

Figure 1. E17.5 *Vax1* KO brains are depleted of GnRH neuron staining. *Vax1* WT, HET, and KO embryos at E13.5, $n = 2–5$ (***A–D***) and E17.5 d, $n = 3–4$ (***E–H***) were processed for IHC staining for GnRH. ***A***, ***E***, Green boxed areas on the drawings of the sagittal mouse head sections to the left of the panels indicate where the ***B*** and ***F*** images were taken. me, Median eminence; pit, pituitary; op, olfactory placode; cp, cribriform plate. The number of GnRH-stained neurons was counted in different subregions of the brain (***C***, ***G***) and in the whole brain (***D***, ***H***). Crib. plate, Cribriform plate; hypo, hypothalamus. Statistical analysis by two-way ANOVA followed by Bonferroni (***C***, ***G***) and one-way ANOVA compared with WT (***D***, ***H***). $*p < 0.05$, $**p < 0.01$, $***p < 0.001$; $n = 3–4$ embryos. Scale bars, 100 μm.

comparable numbers in the nose area in WT and HET mice, whereas a slightly reduced number of GnRH neurons were found in the cribriform plate (crib. plate). Remarkably, only 16% of the expected number of GnRH neurons was detected in the hypothalamic area in *Vax1* HET (Fig. 1*G*). In the entire head, *Vax1* HET mice had a 48% reduction in the number of GnRH neurons (Fig. 1*H*), identifying a dose-dependency on *Vax1* for correct GnRH neuron population maintenance. Furthermore, GnRH staining in the median eminence was decreased in the HET and absent in the KO (Fig. 1*F*). The whole head was systematically analyzed for GnRH neurons, and no ectopic localization of the neurons was observed.

Deletion *of Vax1* in GnRH neurons abolishes GnRH expression

To determine whether the loss of GnRH neurons in *Vax1* KO at E17.5 was due to loss of VAX1 expression within GnRH neurons as opposed to loss of VAX1 expression in the cells of the environment through which they migrate, we generated $Vax1^{flox}$ mice (Fig. 2*A*,*B*) and crossed them with $GnRH^{cre}$ mice (Wolfe et al., 2008), allowing for specific deletion of VAX1 in GnRH neurons. GnRH-expressing neurons were counted in adult $Vax1^{flox/flox}$:$GnRH^{cre}$ mice [conditional KO (cKO)]. Only a couple of GnRH-expressing neurons were identified in the whole cKO brain and no staining at the median eminence was detected (Fig. 2*C*, median eminence). No differences in GnRH neuron counts were observed between males and females and the data were pooled for counts of every second section: control: 275.9 ± 61.8; cKO: 2.8 ± 1.3; Student's *t* test, $p < 0.0003$, $n = 5–6$.

The absence of GnRH staining could arise from either a lack of GnRH gene expression (Livne et al., 1993) or GnRH neuron death (Diaczok et al., 2011). To determine the destiny and timing of the loss of GnRH-expressing cells in the cKO, we first asked whether recombination had taken place at E13.5, a time point when full-body *Vax1* KO embryos had normal GnRH neuron numbers (Fig. 1*D*). To detect recombination, we performed IHC for YFP using the floxed-stop YFP cassette inserted in the ROSA

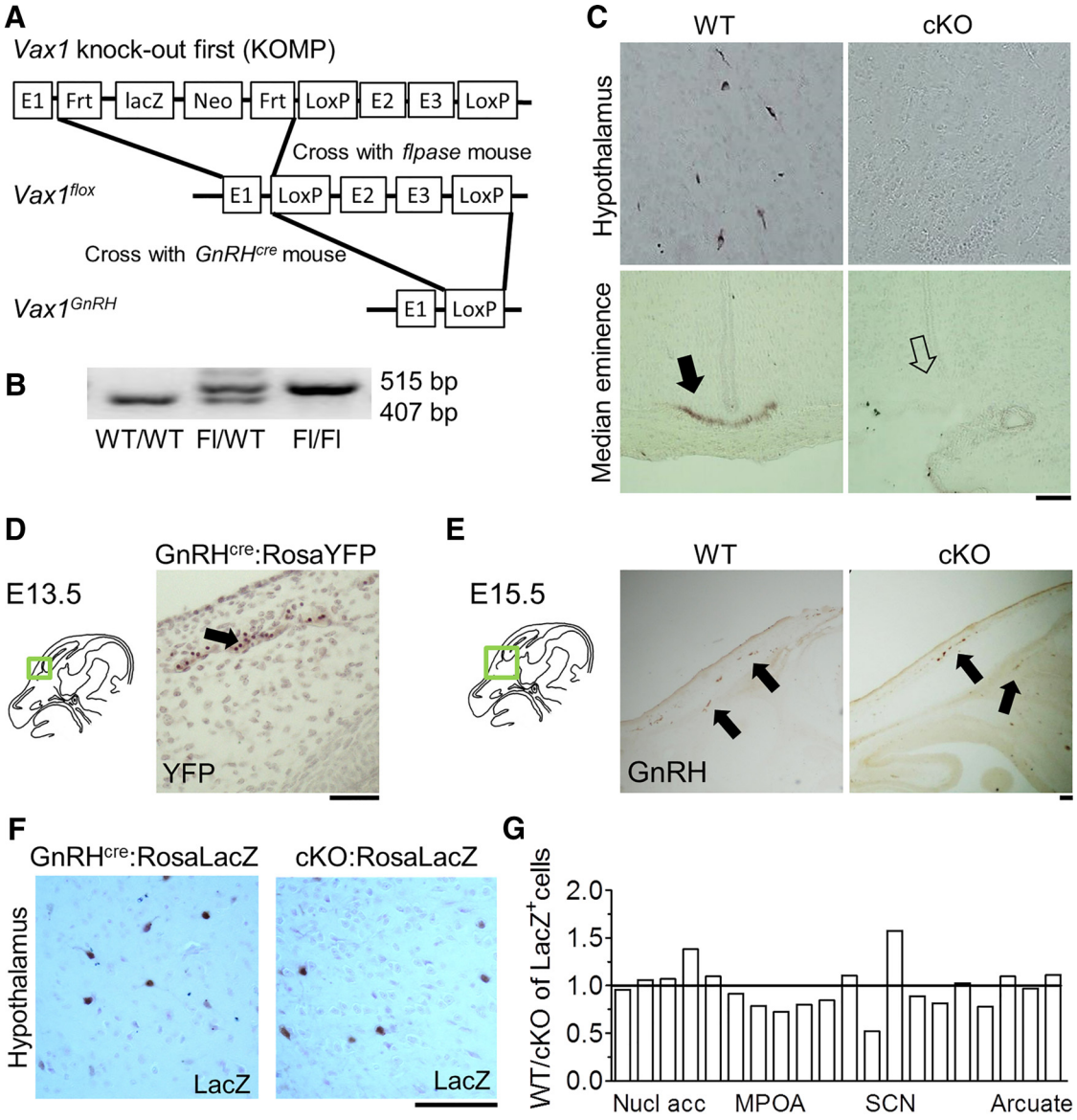

Figure 2. *Vax1*$^{flox/flox}$*:GnRH*^{cre} mice have no GnRH-expressing neurons. ***A***, Strategy for generating the *Vax1*$^{flox/flox}$*:GnRH*^{cre} mouse. The *Vax1 knock-out first* mouse was crossed with a *flpase* mouse to create the conditional allele, then that *Vax1*^{flox} mouse was crossed with a *GnRH*^{cre} mouse to create a homozygous *Vax1*$^{flox/flox}$ with the *GnRH*^{cre} as a heterozygous allele. ***B***, Genotyping for the floxed allele (Fl). ***C***, IHC of GnRH in adult male *Vax1*$^{flox/flox}$ (WT) and *Vax1*$^{flox/flox}$*:GnRH*^{cre} (cKO) mice. Arrow indicates where GnRH staining is expected to be at the median eminence. ***D***, GnRH neuron lineage tracing in *GnRH*^{cre}*:RosaYFP* at E13.5; arrow indicates YFP expression. ***E***, IHC of GnRH in E15.5 WT and cKO; arrows indicate GnRH neurons. Green boxed areas on the drawings of the sagittal mouse head sections to the left of the panels (***D***, ***E***) indicate where the image was taken. ***F***, Lineage tracing in adult female *GnRH*^{cre}*:RosaLacZ* and *Vax1*$^{flox/flox}$*:GnRH*^{cre}*:RosaLacZ* (*cKO:RosaLacZ*) hypothalamus. ***G***, Comparison of *GnRH*^{cre}*:RosaLacZ* driven LacZ-expressing cell localization in WT and *cKO:RosaLacZ* mice ($n = 3$). Nucl acc, Nucleus accumbens; MPOA, medial preoptic area; SCN, suprachiasmatic nucleus. Scale bars, 100 μm.

gene as a Cre-dependent reporter (Srinivas et al., 2001). We detected YFP expression at E13.5, showing recombination in GnRH neurons had taken place (Fig. 2*D*). To establish a time frame for the loss of GnRH expression in cKO mice (Fig. 2*C*), we counted GnRH neurons at E15.5 in WT and cKO mice. In agreement with GnRH neuron numbers in the *Vax1* KO at E13.5 (Fig. 1*D*), we found comparable GnRH neuron numbers in WT and cKO E15.5 embryos (Fig. 2*E*). Every second 10 μm section was counted and stained for GnRH. GnRH neuron numbers were as follows: WT = 538 ± 108, cKO = 415 ± 35, $n = 2$–3; Student's t test, $p = 0.827$). Finally, to determine whether GnRH neurons had died or survived but stopped expressing GnRH in adulthood (Fig. 2*C*), we performed GnRH lineage tracing in mice with *Vax1* deleted in GnRH neurons (*Vax1*$^{flox/flox}$*:GnRH*^{cre}*:Rosa LacZ* mice) and controls (*GnRH*^{cre}*:Rosa LacZ mice*). LacZ staining in the adult brain of *GnRH*^{cre}*:Rosa LacZ* mice and *Vax1*$^{flox/flox}$*:GnRH*^{cre}*:Rosa LacZ* mice was indistinguishable, showing that deletion of *Vax1* in GnRH neurons abolished *Gnrh1* gene expression but that the neurons themselves survive (Fig. 2*F*). To determine whether GnRH neurons migrated differently in the cKO, we evaluated the localization of LacZ expression throughout the brain. We observed GnRH^{cre} driven expression of Rosa LacZ in non-GnRH neuron expressing areas, as previously described for another *GnRH*^{cre} mouse (Yoon et al., 2005), as well as in other unidentified cells (data not shown). Despite this, we were able to determine that there was no difference in GnRH neuron localization in *GnRH*^{cre}*:Rosa LacZ* and *Vax1*$^{flox/flox}$*:GnRH*^{cre}*:Rosa LacZ* mice, with the exception of the area close to the suprachiasmatic nucleus (SCN), where a tendency for GnRH neurons to migrate slightly fur-

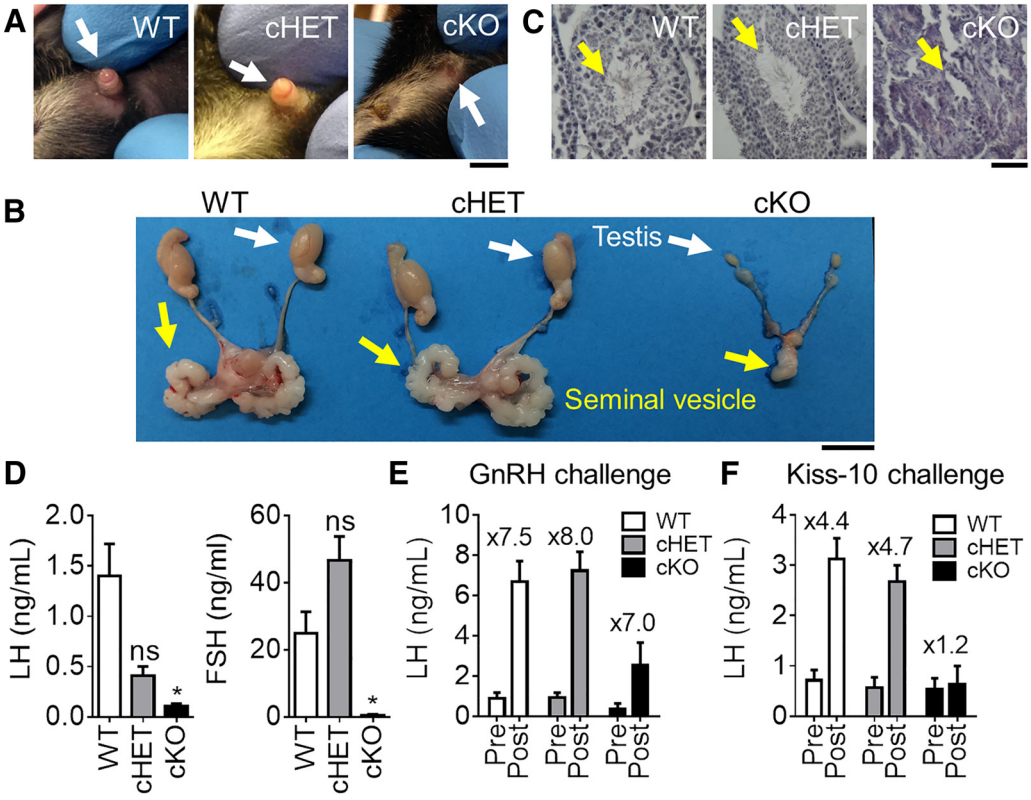

Figure 3. *Vax1*$^{flox/flox}$*:GnRH*^{cre} males have a micropenis and are hypogonadal. ***A***, Image of 6-week-old WT, cHET and cKO males. Scale bar, 0.5 cm. ***B***, Testes of adult mice. Scale bar, 0.5 cm. ***C***, H&E staining of testes from adult WT, cHET, and cKO males. Scale bar, 10 μm. WT and cHET males have a well defined penis (white arrow), preputial separation (WT, cHET), full size testes, seminal vesicles and normal spermatogenesis, whereas cKO have a micropenis (white arrow), delayed preputial separation, very small testes and seminal vesicles, as well as an absence of spermatogenesis. ***D***, Basal circulating LH and FSH levels. One-way ANOVA compared with control. *$p < 0.05$. ***E***, Circulating LH levels after GnRH and (***F***) kisspeptin-10 (kiss-10) challenges. Numbers over the histogram indicate fold-change after GnRH or Kiss-10 challenge; $n = 4–8$.

ther posterior in *Vax1*$^{flox/flox}$*:GnRH*^{cre}*:Rosa LacZ* mice was noted (Fig. 2*F*).

Vax1$^{flox/flox}$*:GnRH*^{cre} mice are hypogonadal

Absence of GnRH or its receptor results in delayed puberty, hypogonadism and infertility because of dramatic reductions in circulating LH and FSH (Gibson et al., 1994; Gill et al., 2008). To assess the impact of lack of GnRH expression in *Vax1*$^{flox/flox}$*:GnRH*^{cre} males (cKO), progression through puberty was assessed. We found that *Vax1*$^{flox/flox}$*:GnRH*^{cre} males had a micropenis (Fig. 3*A*; cKO) and did not achieve puberty, as determined by preputial separation (Korenbrot et al., 1977), or until 56.67 ± 9.60 d of age (no preputial separation observed at 9 weeks of age in 2 of the evaluated males not included in the average; one-way ANOVA, $p = 0.0002$, $n = 3–7$), whereas littermate controls had preputial separation at 30.43 ± 0.75 d of age and cHET males at 29.83 ± 1.3 d of age. As expected, the absence of GnRH-expressing neurons resulted in adult hypogonadism (Fig. 3*B*; cKO), and absence of all stages of spermatogenesis in the testis (Fig. 3*C*, yellow arrow), whereas cHET male testes and seminal vesicles were indistinguishable from WT (Fig. 3*C*). Testicular development relies on LH and FSH release from the pituitary in response to GnRH (Schinckel et al., 1984). Indeed, *Vax1*$^{flox/flox}$*:GnRH*^{cre} males had extremely low circulating FSH and LH levels (Fig. 3*D*). Interestingly, there was a tendency for reduced LH in the cHET males, whereas FSH was close to WT levels (Fig. 3*D*). Finally, to confirm that the lack of circulating LH and FSH originated at the level of the GnRH neurons, we performed GnRH and Kisspeptin (Kiss-10) challenges. The pituitaries of WT, cHET and cKO were able to respond to a GnRH challenge, confirming that the mechanism for low LH was upstream of the pituitary (Fig. 3*E*). However, a kisspeptin challenge, which acts on the KISS1 receptors expressed by GnRH neurons to stimulate GnRH release, was unable to elicit LH increase in the cKO mouse, localizing the defect of pituitary hormone release to the level of the GnRH neuron (Fig. 3*F*).

The fertility of *Vax1*$^{flox/flox}$*:GnRH*^{cre} females was next assessed. *Vax1*$^{flox/flox}$*:GnRH*^{cre} females had delayed vaginal opening (Fig. 4*A*), an external marker of pubertal onset in females. Vaginal opening in WT occurred at 29.29 ± 0.99, cHET females at 30.33 ± 0.67 d of age, whereas opening occurred in cKO at 49.6 ± 5.20 d of age (one-way ANOVA, $p = 0.00041$, $n = 3–7$). The development and function of the ovary relies on LH and FSH release from the pituitary and absence of gonadotropic hormone release leads to hypogonadism (Mason et al., 1986; Gibson et al., 1994). Indeed, *Vax1*$^{flox/flox}$*:GnRH*^{cre} females were hypogonadal (Fig. 4*B*), with an average reduction in ovary size compared with WT of 58% (WT 13.48 ± 2.27 mg; cKO 5.62 ± 2.0 mg; Student's *t* test, $p = 0.026$, $n = 6$). In addition, we observed a 92% reduction in the weight of the uterine horn (WT 73.06 ± 11.93 mg; cKO 5.59 ± 2.72 mg; $n = 6$, Student's *t* test, $p = 0.0003$). Ovarian morphology was evaluated by H&E staining. The WT and cHET mice presented with all the expected stages of follicular development and corpora lutea (CL), an ovarian marker of ovulation (Fig. 4*C*). In contrast, the cKO ovaries had a high accumulation of primary follicles, some presenting with the expected granulosa cell layer (Fig. 4C, black arrows), and some without (Fig. 4*C*, yellow arrows). Late stage primary follicles, secondary follicles,

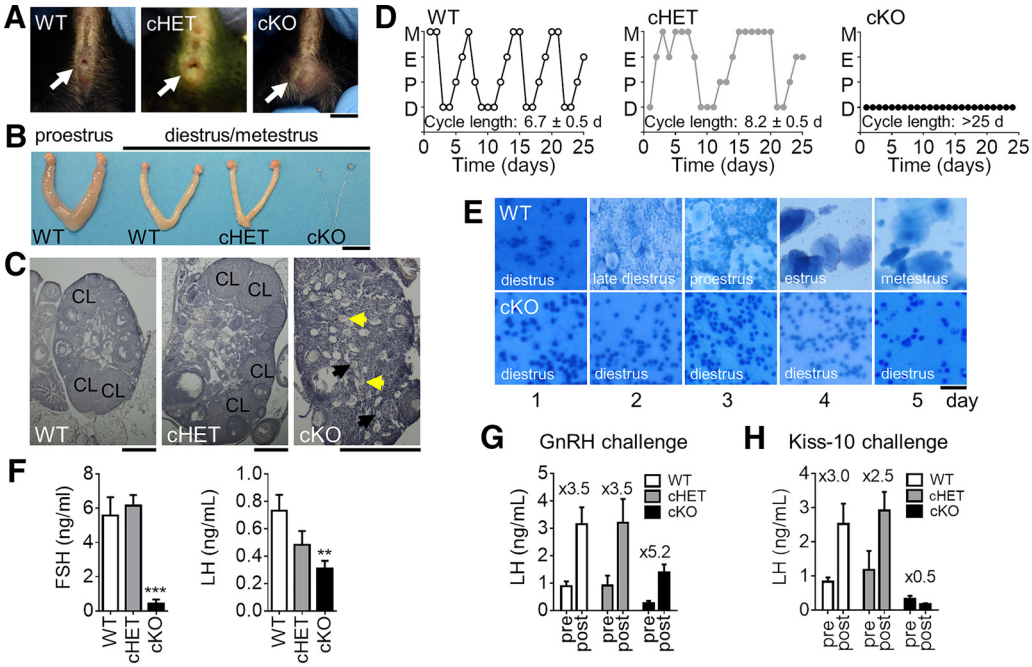

Figure 4. *Vax1*$^{flox/flox}$*:GnRH*^{cre} females have delayed pubertal onset and are hypogonadal. ***A***, Pubertal onset was determined by vaginal opening (WT and cHET, white arrow). Panel shows images of 6-week-old females. Scale bar, 0.5 cm. ***B***, Ovaries and uteri were collected from 25-week-old females. Scale bar, 0.5 cm. ***C***, H&E-stained ovary. CL, Corpora lutea. Black arrows show stage 2 primordial follicles with the expected granulosa cell layer (black arrows), and some without (yellow arrows). Scale bar, 0.5 mm. ***D***, Estrus cycling was monitored daily in adult 12- to 20-week-old WT, cHET, and cKO mice. M, Metestrus; E, estrus; P, proestrus; D, diestrus. ***E***, Representative cell morphology for 5 d in WT and cKO females. ***F***, Diestrus circulating LH and FSH levels. One-way ANOVA; $^{**}p < 0.01$, $^{***}p < 0.001$. Circulating LH levels after (***G***) GnRH and (***H***) kisspeptin-10 (kiss-10) challenges. Numbers over the histograms indicate fold-change after GnRH or Kiss-10 challenge. $n = 6$–11.

and corpora lutea were not observed in the cKO (Fig. 4*C*). The absence of corpora lutea indicates abnormal progression through the estrous cycle and absence of an LH surge. To determine whether cKO females progressed correctly through the estrous cycle, vaginal smears were collected daily for 25 d in adult mice. WT females progressed through the estrous cycle in 5.95 ± 0.31 d ($n = 7$), whereas cHET females required an average of 8.2 ± 0.5 d to complete one cycle ($n = 11$; Fig. 4*D*,*E*). In contrast, cKO females remained in diestrus during the entire 25 d of monitoring (cycle length >25 d, $n = 6$; Fig. 4*D*,*E*). Indeed, circulating diestrus LH and FSH levels were strongly reduced in cKO females compared with WT and cHET females (Fig. 4*F*), indicating an absence of GnRH release at the median eminence. Estrogen levels were assessed in diestrus. Due to the low levels of circulating estrogen in diestrus, none of the cKO samples, and most of the WT and cHET samples were below detection limit of the assay (data not shown). Finally, to confirm that the lack of circulating LH and FSH originated at the level of the GnRH neurons, we performed GnRH and Kisspeptin (Kiss-10) challenges. As expected, LH levels were induced in response to a GnRH challenge (Fig. 4*G*), but not a kisspeptin challenge (Kiss-10; Fig. 4*H*), confirming that the very low levels of circulating LH and FSH were due to a defect in the release of GnRH by GnRH neurons in cKO females.

Finally the fertility of cKO was assessed. Indeed, hypogonadism of males and females led to complete infertility, and no litters were recovered from either cKO males or cKO females each paired with WT mates during a 90 d fertility study, whereas WT to WT matings produced an average of 2.25 ± 0.48 litters in this time frame ($n = 3$–4). Interestingly, there was no obvious infertility phenotype observed when pairing cHET males or females with a WT; however, only one-third of the cHET to cHET matings generated litters within 90 d, indicating that these mice are subfertile.

VAX1 is expressed in GnRH neurons where it directly regulates *Gnrh1* transcription

The absence of GnRH expression in *Vax1*$^{flox/flox}$*:GnRH*^{cre}*:Rosa LacZ* mice, indicates that VAX1 might regulate the GnRH promoter. To explore this possibility, we asked whether *Vax1* was expressed in two model GnRH cell lines, the immature GnRH cells GN11 (Radovick et al., 1991), and the mature GnRH cells GT1-7 (Mellon et al., 1990). We performed qRT-PCR in GN11, GT1-7, and the mouse fibroblast cell line, NIH3T3 (3T3). *Vax1* was highly expressed in GT1-7 cells, whereas no *Vax1* was detected in GN11 or NIH3T3 cells (Fig. 5*A*). Comparable results were confirmed by RNA sequencing in these same cell lines (data not shown). Using a Vax1 siRNA to knock down endogenous *Vax1* from GT1-7 cells, we identified a decrease in *Vax1* transcription at the same time point as an increase in *Gnrh1* transcription (Fig. 5*B*, left; Vax1 knock-down), indicating that VAX1 is a repressor of *Gnrh1* transcription. Consistent with this finding, overexpression of *Vax1* from an expression plasmid transfected into GT1-7 cells repressed endogenous *Gnrh1* levels (Fig. 5*B*, right). In contrast, overexpression of *Vax1* in GN11 cells led to a detectable increase in endogenous *Gnrh1* (Fig. 5*B*, right; *Vax1* overexpression). It should be noted that although GN11 and GT1-7 cells are excellent *in vitro* models of immature and mature GnRH neurons, respectively, these remain cell lines that may not recapitulate all of the characteristics of GnRH neurons *in vivo*. However, these cell lines are very useful tools to understand gene transcription regulation in GnRH neurons and to advance our understanding of GnRH neuron function.

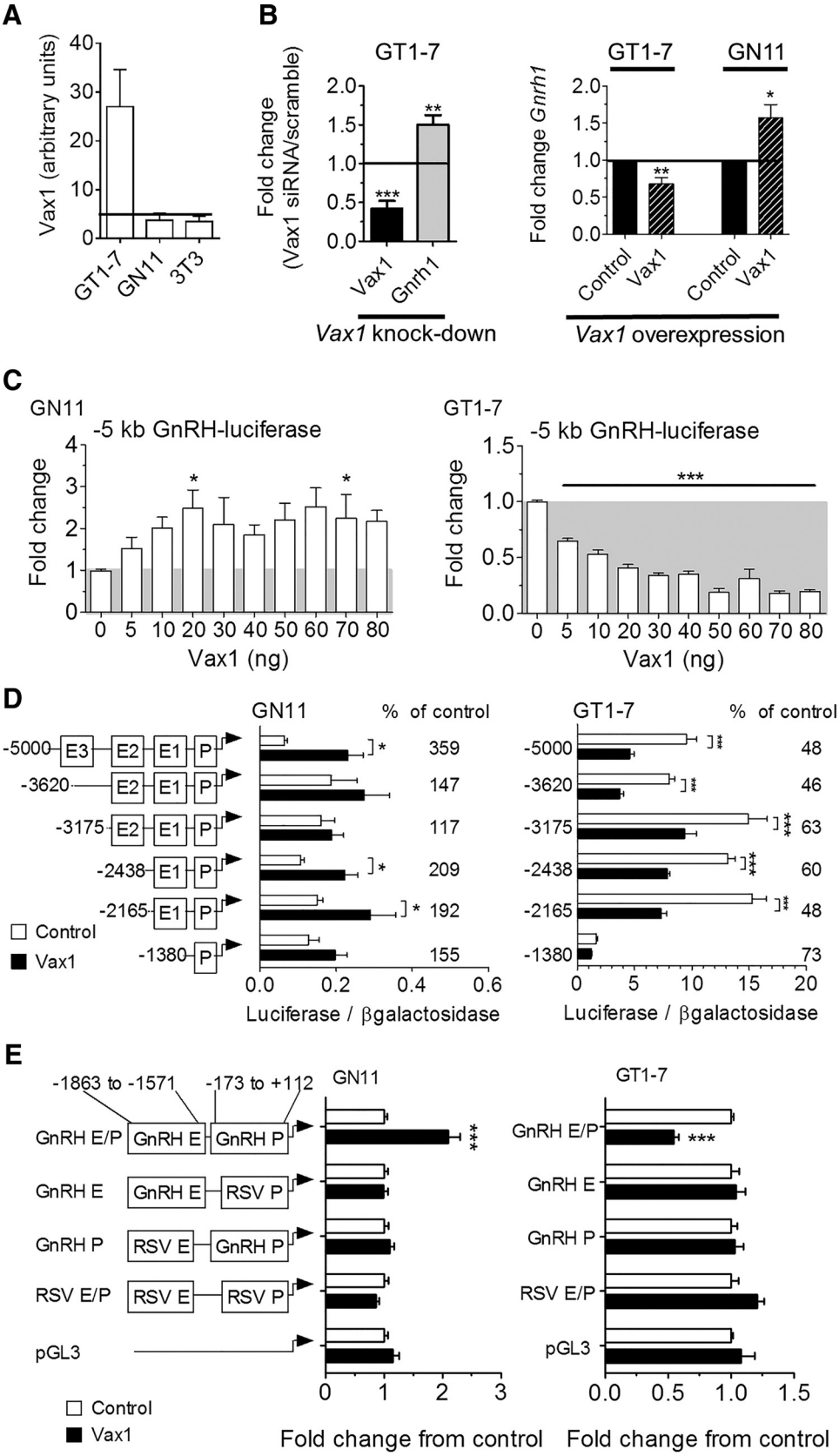

Figure 5. VAX1 regulates *Gnrh1* transcription through the GnRH enhancer 1 and promoter. Levels of *Vax1* mRNA were determined by ***A,*** qRT-PCR in a mature GnRH cell line (GT1-7), an immature GnRH cell line (GN11), and NIH3T3 fibroblasts (3T3). The horizontal bar indicates lowest detectable RNA level. $n = 6-8$. ***B***, GT1-7 cells were transfected with siRNA containing a scrambled or Vax1 sequence. Endogenous RNA levels of *Vax1* or *Gnrh1* were determined by qRT-PCR. Data represent fold-change compared with scrambled siRNA; $N = 3–5$ in duplicates. Statistical analysis by Student's *t* test compared with control. $^*p < 0.05$, $^{**}p < 0.01$. ***C***, Left, GT1-7 cells were transfected with a *Vax1*-expression vector (Vax1, black hatched) and its empty vector (control, black). Right, GN11 cells were transfected with *Vax1*-expression vector (Vax1, black hatched) and its empty vector (control, black). Data represent fold-change compared with (*Figure legend continues.*)

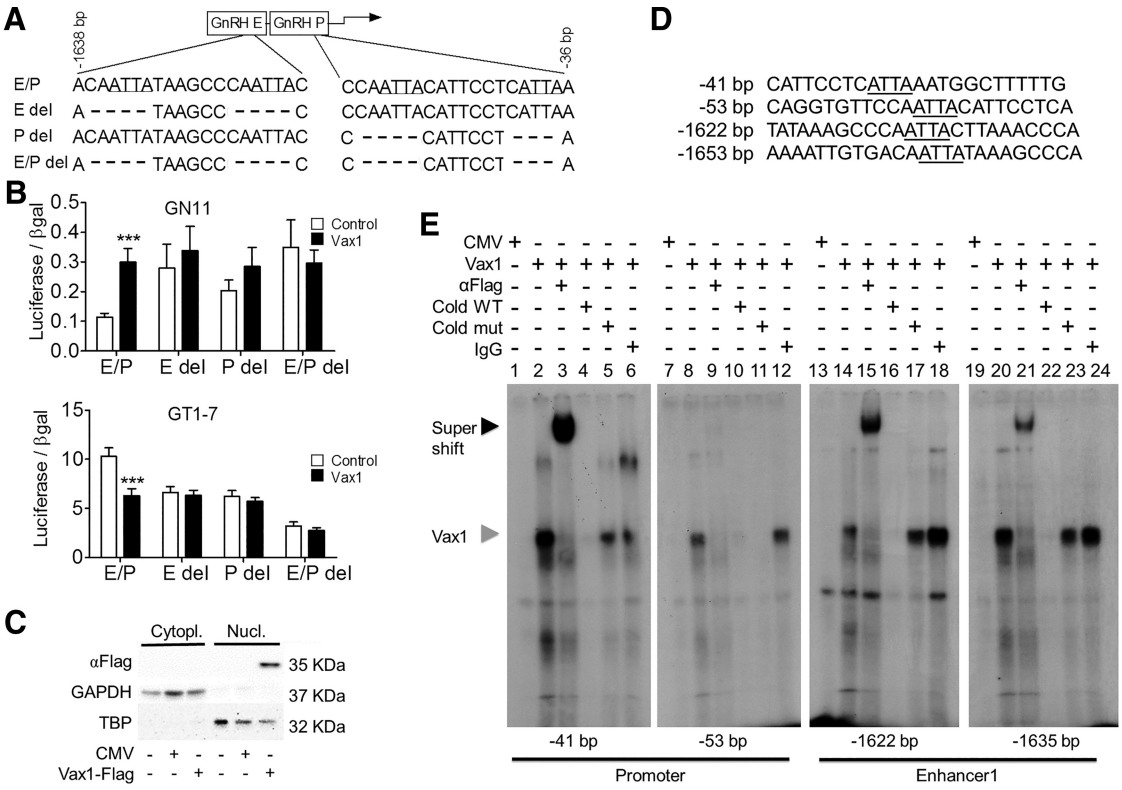

Figure 6. VAX1 regulates GnRH transcription through direct binding to ATTA sites in the GnRH-E1 and proximal promoter (P). ***A***, Deletion of potential ATTA binding sites of VAX1 within the GnRH enhancer1/promoter (GnRH-E/P or E/P). ***B***, Cotransfection of the indicated luciferase reporters with (black) or without (white) 10 ng of Vax1 in GN11 and GT1-7 cells. Data are expressed as fold-induction compared with GnRH E/P. Statistical analysis by two-way ANOVA followed by Bonferroni. ***$p < 0.001$ compared with control. ***C***, COS-1 cells were transiently transfected with a *Vax1*-flag expression vector or its empty vector, CMV, and harvested 24 h post-transfection. Western blot shows detection of VAX1-flag, GAPDH (glyceraldehyde-3phosphate dehydrogenase), and TBP in the nucleus (Nucl) versus the cytoplasm (Cytopl). ***D***, Probe sequences used for EMSA covering the ATTA sites found to be involved in VAX1 regulation of *Gnrh1* transcription (sites indicated in ***A***). The underlined ATTA elements were converted to GCCG in the mutant probes (Cold mut). ***E***, EMSA performed using nuclear extracts from COS-1 cells transfected with *Vax1*-flag plasmid or control expression vector. Black arrowhead indicates super shift, gray arrowhead indicates origin of supershifted band. Wild-type (Cold WT) and mutant (Cold mut) probes were used at 100-fold higher concentration than labeled WT probe.

To identify the region of the GnRH promoter where VAX1 acts, we used a 5 kb rat GnRH promoter driving luciferase. A dose–response study was conducted by cotransfecting the 5 kb GnRH promoter into GN11 and GT1-7 cells with increasing *Vax1* concentrations. Twenty-one hours after transfection, VAX1 increased GnRH-promoter driven luciferase transcription in GN11 cells and reached maximal effect at 20 ng of *Vax1* (Fig. 5*C*, left). In contrast, VAX1 repressed *Gnrh1* transcription in GT1-7 cells (Fig. 5*C*, right). Maximal repression was observed at 50 ng of *Vax1* (Fig. 5*C*). To avoid nonspecific transcriptional effects due to an excessive amount of VAX1, we chose to conduct further studies with 10 or 20 ng, producing ~70% of the maximal effect. Interestingly, VAX1 regulated the *Gnrh1* promoter oppositely in the two GnRH cell lines depending on their state of maturation, perhaps since GT1-7 cells have ample endogenous *Vax1*, whereas GN11 cells lack *Vax1* entirely. Another possible explanation for this difference could be that VAX1 uses different binding sites in the *Gnrh1* promoter to regulate transcription at different developmental stages. A characteristic of homeodomain proteins is their capacity to bind ATTA sites in the promoter region of their target genes. We identified numerous ATTA and ATTAA sequences in the 5 kb GnRH promoter region. To narrow down the potential binding sites for VAX1, we used a series of 5′ truncations of the 5 kb GnRH promoter (Fig. 5*D*; Iyer et al., 2010). In GN11 cells, elimination of enhancer 3 (E3) abolished the capacity of VAX1 to regulate transcription (Fig. 5*D*, left). However, elimination of enhancer 2 (E2) restored induction of transcription by VAX1 on both the −2438 and −2168 bp reporters, suggesting that E3 contains sites that affect VAX1-mediated transcription. Further, the effect of VAX1 on the −1380 bp reporter was reduced to the extent that it did not reach significance (Student's *t* test, $p = 0.1032$). This suggests that enhancer 1 (E1) is necessary for VAX1 enhanced transcription of GnRH in GN11 cells. In GT1-7 cells, VAX1 repression of GnRH transcription was maintained on all of the truncated reporters, except the −1380 bp (Fig. 5*D*, right), although with slightly different efficiencies (Fig.

←

(*Figure legend continued.*) empty vector. Statistical analysis by Student's *t* test compared with control. *$p < 0.05$, **$p < 0.01$. ***C***, GN11 and GT1-7 cells were cotransfected with a luciferase reporter driven by the 5 kb promoter region of the rat GnRH gene and increasing concentrations of *Vax1*. All samples were transfected with equal amounts of DNA by using the empty CMV vector. Statistical analysis by one-way ANOVA followed by Tukey *post hoc*. *$p < 0.05$, ***$p < 0.001$. ***D***, Cotransfection with 5′ truncations of the GnRH 5 kb promoter driving luciferase with (black) or without (white) 10 ng of *Vax1*. Luciferase data are expressed as fold-induction compared with pGL3. The percentage change between cotransfection with 0 versus 10 ng of *Vax1* on the reporters is indicated on the graph. Statistical analysis by two-way ANOVA followed by Dunnett's multiple comparison. *$p < 0.05$, **$p < 0.01$, ***$p < 0.001$. ***E***, Vax1 regulation of the RSV enhancer/promoter (RSV E/P) driving luciferase with or without the GnRH enhancer 1 (GnRH E, −1863 to −1571 bp) or GnRH promoter (GnRH P −173 to +112 bp). Data are expressed as fold-induction compared with empty vector for each reporter. Statistical analysis by Student's *t* test. ***$p < 0.001$. Luciferase transfection studies represent $n = 3$–5 performed in triplicate.

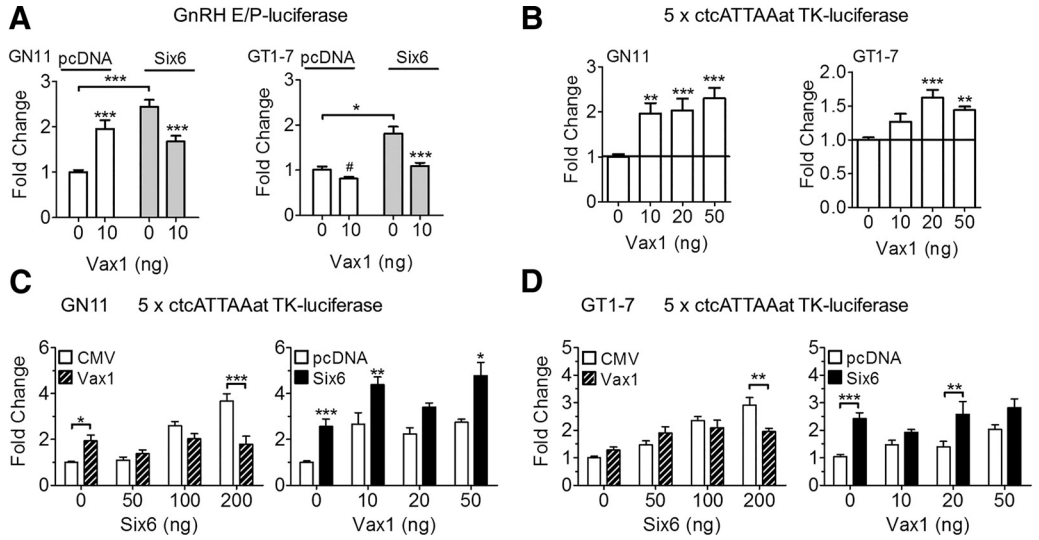

Figure 7. VAX1 and SIX6 compete for regulation of the *Gnrh1* promoter. ***A***, GN11 and GT1-7 cells were cotransfected with or without *Six6* (as noted on figure or 200 ng) or *Vax1* (as noted on figure or 20 ng). Transcriptional activity was evaluated using the GnRH-E/P-luciferase reporter or (***B–D***) using the 5× ctcATTAat-TK-luciferase multimer reporter. Statistical analysis was by two-way ANOVA followed by *post hoc* Bonferroni. Fold-changes are compared with control (0 ng *Vax1*, 0 ng *Six6*) or as indicated by bar. $*p < 0.05$, $**p < 0.01$, $***p < 0.001$. Student's *t* test compared with control. $\#p < 0.05$. Horizontal line indicates control level. All experiments were performed in triplicate and repeated three to six times.

5*D*, right). These data indicate that VAX1 requires GnRH-E1 to modulate GnRH transcription in both cell lines. To determine whether VAX1 regulates transcription through both E1 and P or E1 alone, we tested the capacity of VAX1 to mediate transcription of the GnRH-E1 or GnRH-P separately using the Rous sarcoma virus promoter (RSVp) or RSV enhancer (RSVe) to help drive transcription (Fig. 5*E*). In both GN11 and GT1-7 cells, the separation of GnRH-E1 from the GnRH-P abolished the regulation of VAX1 on transcription (Fig. 5*E*). Therefore, VAX1 requires both the GnRH enhancer 1 and promoter to regulate *Gnrh1* transcription.

We have previously shown that ATTA sites within E1 and P of the GnRH regulatory region are involved in induction by homeodomain proteins SIX6 and DLX, and repression by MSX, of GnRH transcription (Givens et al., 2005; Larder et al., 2011). Based on these data, we hypothesized that VAX1 was likely to regulate GnRH transcription through these same sites. Cotransfection of GN11 and GT1-7 cells with *Vax1* and GnRH-luciferase reporters with or without ATTA deletions in P and E1 (Fig. 6*A*), confirmed that VAX1 required the two pairs of ATTA binding sites in E1 and P to regulate GnRH transcription in both cell lines (Fig. 6*B*). To identify to which of the four ATTA sites in the GnRH-E1/P (Fig. 6*A*) VAX1 directly binds, we performed EMSAs with radioactively labeled probes (Fig. 6*D*). COS-1 cells transiently transfected with a *Vax1*-flag overexpression vector contained high levels of VAX1-flag protein (Fig. 6*C*), which was exclusively localized in the nuclear fraction of the cell lysate. This exclusive nuclear localization of VAX1 in COS-1 cells, contrasts with what others have described for VAX1 (Kim et al., 2014). Nuclear extracts from COS-1 cells transiently transfected with *Vax1*-flag formed a complex (Fig. 6*E*, gray arrowhead) that was supershifted (Fig. 6*E*, black arrowhead) in presence of a flag antibody (lanes 3, 15, and 21). In contrast to addition of excess unlabeled mutant probe (ATTA sequence mutated to GCCG; Fig. 6D, underlined sequence and lanes 6, 12, 18, and 24, Cold mut, gray arrow), addition of excess WT probe decreased complex formation and competed away VAX1 binding to the probe (Cold WT, lanes 5, 11, 17, and 23, gray arrow).

VAX1 competes with homeodomain SIX6 for ATTA sites in the *Gnrh1* promoter

The transfection studies identified VAX1 as a strong positive regulator of the *Gnrh1* promoter in GN11, and a repressor in GT1-7 (Figs. 5, 6). VAX1-regulated transcription was mediated by binding to four sites in the proximal *Gnrh1* promoter: −41, −53, −1622, and −1635 bp (Fig. 6*E*). Some of these sites are known to be bound by other homeodomain proteins regulating the *Gnrh1* promoter, such as SIX6 (Larder et al., 2011). Like VAX1, SIX6 is not expressed in GN11, and highly expressed in GT1-7, where it is a strong activator of the *Gnrh1* promoter (Larder et al., 2011). We hypothesized that VAX1 was an activator in both GN11 and GT1-7. However, if VAX1 has a higher affinity than SIX6 for the *Gnrh1* promoter but is a weaker activator, then that would enable VAX1 to displace SIX6 (a strong activator), thus making it appear as if VAX1 was a repressor. To test this hypothesis, we investigated whether VAX1 could compete with SIX6 for binding to the *Gnrh1* promoter. As both SIX6 (Larder et al., 2011) and VAX1 bind in the *Gnrh1* promoter and E1 (Fig. 6), we studied the effects of VAX1 and SIX6 on the GnRH E1-P-luciferase reporter. In GN11 cells, VAX1 and SIX6 alone each increased transcription (Fig. 7*A*, GN11). Cotransfection of *Vax1* and *Six6* revealed a level of transcription comparable to *Vax1* alone (Fig. 7*A*, GT1-7), indicating that the effect observed was principally mediated by VAX1 and not SIX6. In GT1-7 cells, VAX1 repressed, whereas SIX6 activated, transcription (Fig. 7*A*, right). Cotransfection of *Vax1* and *Six6* led to a level of transcription close to that of *Vax1* alone, suggesting that the effect observed was mediated by VAX1. To further support that VAX1 is a positive regulator of the *Gnrh1* promoter in mature GnRH neurons, we used an ATTA multimer driving luciferase. In GN11 cells, VAX1 increased transcription at all concentrations studied (Fig. 7*B*, GN11). Interestingly, VAX1 proved to be a weak positive activator of the ATTA multimer in GT1-7 cells (Fig. 7*B*, GT1-7). To evaluate whether VAX1 and SIX6 do indeed compete for binding to ATTA sites, we evaluated transcriptional activity by performing SIX6 and VAX1 cotransfections with increasing concentrations of one or the other transcription factor. As expected, SIX6 strongly increased transcription of the ATTA multimer in both cell lines, whereas VAX1

was a strong activator in GN11 and weak activator in GT1-7 (Fig. 7*C*, GN11, *D*, GT1-7). In the presence of increasing concentrations of SIX6, *Vax1*-induced (20 ng) ATTA transcription levels were comparable to VAX1 alone in both GN11 and GT1-7 (Fig. 7*C*,*D*, left). Interestingly, increasing concentrations of *Vax1* were not able to consistently reduce SIX6-induced (200 ng) transcription (Fig. 7*C*,*D*, right), indicating that VAX1 is a positive regulator of the *Gnrh1* promoter, and competes with the binding of SIX6 to ATTA sites to regulate *Gnrh1* transcription thus resulting in reduced *Gnrh1* transcription by replacing a stronger activator (SIX6) with a weaker one (VAX1).

Discussion

VAX1 expression in GnRH neurons determines their fate

The physiology of fertility is particularly complex due to the numerous organs, hormones and timing required for its maintenance (Beaver et al., 2002; Boden and Kennaway, 2005, 2006; Williams et al., 2007). Infertility originating at the level of GnRH neurons frequently arises from a disruption of their maturation or migration during development (Pitteloud et al., 2006; Schwarting et al., 2007). Homeodomain transcription factors are known to be modulators of GnRH neuron maturation and mutations in, for example, *Six6*, *Vax1*, or *Otx2*, cause various degrees of infertility due to abnormal GnRH neuron development (Diaczok et al., 2011; Larder et al., 2011, 2013; Hoffmann et al., 2014).

In the current study, we determined the role of VAX1 in GnRH neurons and in fertility. We demonstrate *Vax1* expression in GnRH neurons and find that during early GnRH neuron development (E13.5), the absence of VAX1 (*Vax1* KO) does not impact GnRH neuron generation, but has a crucial role in the maintenance of GnRH expression at E17.5. Interestingly, the *Vax1* HET mouse at E17.5 had an ~50% reduction in GnRH neurons, showing that *Vax1* dosage is crucial in GnRH neuron development, and that the decrease in GnRH neurons in adulthood (Hoffmann et al., 2014) originates between E13.5 and E17.5.

To understand the role of VAX1 within GnRH neurons in development, we generated $Vax1^{flox}$ mice and crossed them with $GnRH^{cre}$ mice. Deletion of *Vax1* in GnRH neurons (cKO) resulted in a 99% reduction of GnRH-expressing neurons in adulthood, without affecting GnRH neuron numbers at E15.5. In contrast to the death of GnRH neurons observed by lineage tracing in mice with *Otx2* deleted in GnRH neurons (Diaczok et al., 2011) or in the *Six6* KO mouse (unpublished), lineage tracing in $Vax1^{flox/flox}$:$GnRH^{cre}$:*Rosa LacZ* mice revealed that GnRH neurons remained alive, and had migrated correctly to the hypothalamus, but no longer expressed GnRH, involving VAX1 in the maturation of GnRH neurons, and the maintenance of expression of GnRH into adulthood. The absence of GnRH expression led to delayed puberty, hypogonadism, extremely low circulating gonadotropin levels, and complete infertility in both sexes. In agreement with our findings in the *Vax1* HET mouse (Hoffmann et al., 2014), the cHET had a very modest subfertility phenotype. The cHET mice were comparable to WT in all fertility studies, with the exception that cHET females had slightly reduced circulating LH and cHET to cHET matings were subfertile. This suggests that dosage of *Vax1* within GnRH neurons is important for GnRH neuron development and that the cHET mouse reproduces most of the phenotypes seen in the global *Vax1* HET (Hoffmann et al., 2014). However, as not all of the data were equivalent to the *Vax1* HET, it is likely that *Vax1* expressed by other cell types along the migratory route or in the preoptic area of the hypothalamus might also influence the reproductive axis. Alternatively, *Vax1* could be important for the function of anteroventral periventricular nucleus kisspeptin neurons (see below; Hoffmann et al., 2014).

In the brain, kisspeptin and GnRH neurons are key for progression through puberty and maintenance of fertility (Kauffman, 2010; Kim et al., 2013). Kisspeptin neurons localized in the anteroventral periventricular nucleus stimulate GnRH neurons to release GnRH by acting on the KISS1 receptor. Absence of kisspeptin or the KISS1 receptor, leads to complete infertility due to lack of GnRH neuron stimulation of gonadotropes (Lapatto et al., 2007; Clarkson et al., 2008; Pielecka-Fortuna et al., 2008; Kirilov et al., 2013). It has previously been shown that kisspeptin stimulation of GnRH neurons *in vitro* leads to an opening of *Gnrh1* chromatin structure, increasing recruitment of the transcription factor OTX2, an activator of *Gnrh1* transcription (Novaira et al., 2015).

To confirm that the reproductive incompetence of cKO mice arises at the level of GnRH neurons, we challenged both sexes with injections of GnRH or kisspeptin. The capacity of GnRH, but not kisspeptin, to elicit an increase in circulating LH, confirmed that low gonadotropin levels in the cKO mice was not due to a lack of responsiveness of the pituitary to GnRH, but the complete absence of GnRH input to this structure. As the $GnRH^{cre}$ targets GnRH neurons (Wolfe et al., 2008), and we observe a >99% reduction of GnRH neuron staining, this study confirms that the absence of GnRH expression in hypothalamic neurons in the cKO mice is the origin of infertility.

Maintenance of GnRH expression depends on competition between binding by VAX1 and SIX6 to the *Gnrh1* promoter

The 5 kb *Gnrh1* promoter region is well characterized and has been shown to contain three evolutionarily conserved enhancer regions: E3 (−3952 to −3895 bp), E2 (−3135 to −2631 bp), and E1 (−1863 to −1571 bp; Whyte et al., 1995; Iyer et al., 2010), in addition to the conserved proximal promoter (173 bp to +1). The specific neuronal expression of GnRH *in vivo* only requires the proximal GnRH, E1 and P (Lawson et al., 2002). Consequently, the coordinated binding of transcription factors to GnRH-E1 and GnRH-P is tightly associated with specificity of *Gnrh1* transcription, as confirmed by our study. The 5 kb region upstream of the *Gnrh1* transcriptional start site contains numerous potential binding sites for homeodomain proteins (Larder and Mellon, 2009; Larder et al., 2011; Novaira et al., 2012). To investigate the role of VAX1 on the *Gnrh1* promoter and enhancers, we studied transcriptional regulation in the two GnRH cell lines, GN11 and GT1-7. The developmental stage of GnRH neurons at E13.5 is thought to closely mimic the maturation stage of GN11 cells, whereas GT1-7 cells reflect a more mature, postmigratory GnRH neuron. Our data suggest that *Vax1* expression is activated during the migration of GnRH neurons between E13.5 and E17.5 and is required for maintaining expression of GnRH in this neuronal population after E15.5. We found that VAX1 is a repressor of the 5 kb GnRH promoter in GT1-7 cells, but an inducer in GN11 cells. The differential regulation of the 5 kb GnRH promoter was not due to the use of different binding sites by VAX1 in the two cell lines. Due to our inability to validate any commercially available VAX1 antibodies for EMSA or ChIP assays, we used COS-1 cells transient transfected with VAX1-flag to determine whether VAX1 directly interacts with the identified ATTA sites of the *Gnrh1* promoter and enhancer. Using this approach, we identified a strong interaction of VAX1 on the −1622 and −1635 bp sites in E1 and on the −41 site in P, and a weak interaction at −53. These sites have previously been described to

be bound by homeodomain transcription factors such as SIX6 (Larder et al., 2011), MSX1/2 and DLX1/2/5 (Givens et al., 2005). The expression levels of these transcription factors, along with VAX1, are different between GN11 and GT1-7 cells. We hypothesized that a specific balance of transcription factors, their specific promoter occupancy, activational capacity, and binding affinities would determine whether an induction or repression of *Gnrh1* transcription occurred (Givens et al., 2005; Rave-Harel et al., 2005; Larder et al., 2011). We found that the repression of *Gnrh1* transcription in GT1-7 cells by VAX1, in fact, reflects the capacity of VAX1 to displace a strong activator from the promoter, such as SIX6. Replacing a strong activator (SIX6) with a weak activator (VAX1) would result in a decrease in transcription. Our data identified VAX1 as a weak activator on an ATTA-multimer, showing that VAX1 is an activator of transcription in both GN11 and GT1-7. Competition studies between VAX1 and SIX6 on the ATTA-multimer revealed a complex interplay between these two transcription factors. Depending on the specific concentration of each transcription factor, ATTA-luciferase transcriptional levels changed. This suggests that a specific balance of SIX6 and VAX1 elicits different transcriptional activities of the *Gnrh1* promoter, a concept also supported by the dose dependence on *Vax1 in vivo*. These two transcription factors most likely compete with other homeodomain transcription factors, highlighting the complexity of *Gnrh1* transcription regulation. Overall, we found that VAX1 is an activator of the *Gnrh1* promoter, but depending on the concentration and localization of other homeodomain transcription factors, such as SIX6, its overall effect on *Gnrh1* transcription is to increase or decrease transcription levels. The strong activation of the *Gnrh1* promoter in GN11 cells also indicates that VAX1 is important for increasing *Gnrh1* expression during GnRH neuron maturation, which might be the origin of the loss of GnRH expression in the adult cKO mouse. Another possibility is that deletion of *Vax1* from GnRH neurons during development leads to an imbalance of transcription factors regulating the *Gnrh1* promoter, as well as other genes important for GnRH neuron maturation, leading to an almost complete absence of GnRH-expressing neurons in adulthood.

In conclusion, our findings identify a critical role for VAX1 in GnRH neuron maturation, where it is required for the maintenance of GnRH expression through direct binding to the *Gnrh1* promoter. Lack of VAX1 in embryonic development disrupts continuation of GnRH expression after E15.5, and leads to hypogonadism and complete infertility.

References

Beaver LM, Gvakharia BO, Vollintine TS, Hege DM, Stanewsky R, Giebultowicz JM (2002) Loss of circadian clock function decreases reproductive fitness in males of *Drosophila* melanogaster. Proc Natl Acad Sci U S A 99:2134–2139. CrossRef Medline

Bertuzzi S, Hindges R, Mui SH, O'Leary DD, Lemke G (1999) The homeodomain protein vax1 is required for axon guidance and major tract formation in the developing forebrain. Genes Dev 13:3092–3105. CrossRef Medline

Bharti K, Gasper M, Bertuzzi S, Arnheiter H (2011) Lack of the ventral anterior homeodomain transcription factor VAX1 leads to induction of a second pituitary. Development 138:873–878. CrossRef Medline

Bianco SD, Kaiser UB (2009) The genetic and molecular basis of idiopathic hypogonadotropic hypogonadism. Nat Rev Endocrinol 5:569–576. CrossRef Medline

Boden MJ, Kennaway DJ (2005) Reproduction in the arrhythmic *Bmal1* knockout mouse. Reprod Fertil Dev 17:126. CrossRef

Boden MJ, Kennaway DJ (2006) Circadian rhythms and reproduction. Reproduction 132:379–392. CrossRef Medline

Chan YM, de Guillebon A, Lang-Muritano M, Plummer L, Cerrato F, Tsiaras S, Gaspert A, Lavoie HB, Wu CH, Crowley WF Jr, Amory JK, Pitteloud N, Seminara SB (2009) GNRH1 mutations in patients with idiopathic hypogonadotropic hypogonadism. Proc Natl Acad Sci U S A 106:11703–11708. CrossRef Medline

Clarkson J, d'Anglemont de Tassigny X, Moreno AS, Colledge WH, Herbison AE (2008) Kisspeptin-GPR54 signaling is essential for preovulatory gonadotropin-releasing hormone neuron activation and the luteinizing hormone surge. J Neurosci 28:8691–8697. CrossRef Medline

Diaczok D, DiVall S, Matsuo I, Wondisford FE, Wolfe AM, Radovick S (2011) Deletion of Otx2 in GnRH neurons results in a mouse model of hypogonadotropic hypogonadism. Mol Endocrinol 25:833–846. CrossRef Medline

Dodé C, Teixeira L, Levilliers J, Fouveaut C, Bouchard P, Kottler ML, Lespinasse J, Lienhardt-Roussie A, Mathieu M, Moerman A, Morgan G, Murat A, Toublanc JE, Wolczynski S, Delpech M, Petit C, Young J, Hardelin JP (2006) Kallmann syndrome: mutations in the genes encoding prokineticin-2 and prokineticin receptor-2. PLoS Genet 2:e175. CrossRef Medline

Gibson MJ, Kasowski H, Dobrjansky A (1994) Continuous gonadotropin-releasing hormone infusion stimulates dramatic gonadal development in hypogonadal female mice. Biol Reprod 50:680–685. CrossRef Medline

Gill JC, Wadas B, Chen P, Portillo W, Reyna A, Jorgensen E, Mani S, Schwarting GA, Moenter SM, Tobet S, Kaiser UB (2008) The gonadotropin-releasing hormone (GnRH) neuronal population is normal in size and distribution in GnRH-deficient and GnRH receptor-mutant hypogonadal mice. Endocrinology 149:4596–4604. CrossRef Medline

Givens ML, Rave-Harel N, Goonewardena VD, Kurotani R, Berdy SE, Swan CH, Rubenstein JL, Robert B, Mellon PL (2005) Developmental regulation of gonadotropin-releasing hormone gene expression by the MSX and DLX homeodomain protein families. J Biol Chem 280:19156–19165. CrossRef Medline

Hallonet M, Hollemann T, Wehr R, Jenkins NA, Copeland NG, Pieler T, Gruss P (1998) Vax1 is a novel homeobox-containing gene expressed in the developing anterior ventral forebrain. Development 125:2599–2610. Medline

Hallonet M, Hollemann T, Pieler T, Gruss P (1999) Vax1, a novel homeobox-containing gene, directs development of the basal forebrain and visual system. Genes Dev 13:3106–3114. CrossRef Medline

Herbison AE, Porteous R, Pape JR, Mora JM, Hurst PR (2008) Gonadotropin-releasing hormone (GnRH) neuron requirements for puberty, ovulation and fertility. Endocrinology 149:597–604. CrossRef Medline

Hoffmann HM, Tamrazian A, Xie H, Pérez-Millán MI, Kauffman AS, Mellon PL (2014) Heterozygous deletion of ventral anterior homeobox (Vax1) causes subfertility in mice. Endocrinology 155:4043–4053. CrossRef Medline

Iyer AK, Miller NL, Yip K, Tran BH, Mellon PL (2010) Enhancers of GnRH transcription embedded in an upstream gene use homeodomain proteins to specify hypothalamic expression. Mol Endocrinol 24:1949–1964. CrossRef Medline

Kauffman AS (2010) Coming of age in the kisspeptin era: sex differences, development, and puberty. Mol Cell Endocrinol 324:51–63. CrossRef Medline

Kim J, Tolson KP, Dhamija S, Kauffman AS (2013) Developmental GnRH signaling is not required for sexual differentiation of kisspeptin neurons but is needed for maximal Kiss1 gene expression in adult females. Endocrinology 154:3273–3283. CrossRef Medline

Kim N, Min KW, Kang KH, Lee EJ, Kim HT, Moon K, Choi J, Le D, Lee SH, Kim JW (2014) Regulation of retinal axon growth by secreted Vax1 homeodomain protein. Elife 3:e02671. CrossRef Medline

Kirilov M, Clarkson J, Liu X, Roa J, Campos P, Porteous R, Schütz G, Herbison AE (2013) Dependence of fertility on kisspeptin-Gpr54 signaling at the GnRH neuron. Nat Commun 4:2492. Medline

Korenbrot CC, Huhtaniemi IT, Weiner RI (1977) Preputial separation as an external sign of pubertal development in the male rat. Biol Reprod 17:298–303. CrossRef Medline

Lapatto R, Pallais JC, Zhang D, Chan YM, Mahan A, Cerrato F, Le WW, Hoffman GE, Seminara SB (2007) Kiss1$^{-/-}$ mice exhibit more variable hypogonadism than Gpr54$^{-/-}$ mice. Endocrinology 148:4927–4936. CrossRef Medline

Larder R, Mellon PL (2009) Otx2 induction of the gonadotropin-releasing

hormone promoter is modulated by direct interactions with Grg co-repressors. J Biol Chem 284:16966–16978. CrossRef Medline

Larder R, Clark DD, Miller NL, Mellon PL (2011) Hypothalamic dysregulation and infertility in mice lacking the homeodomain protein Six6. J Neurosci 31:426–438. CrossRef Medline

Larder R, Kimura I, Meadows J, Clark DD, Mayo S, Mellon PL (2013) Gene dosage of Otx2 is important for fertility in male mice. Mol Cell Endocrinol 377:16–22. CrossRef Medline

Lawson MA, Macconell LA, Kim J, Powl BT, Nelson SB, Mellon PL (2002) Neuron-specific expression *in vivo* by defined transcription regulatory elements of the GnRH gene. Endocrinology 143:1404–1412. CrossRef Medline

Livak KJ, Schmittgen TD (2001) Analysis of relative gene expression data using real-time quantitative PCR and the $2^{-\delta\delta CT}$ method. Methods 25:402–408. CrossRef Medline

Livne I, Gibson MJ, Silverman AJ (1993) Gonadotropin-releasing hormone (GnRH) neurons in the hypogonadal mouse elaborate normal projections despite their biosynthetic deficiency. Neurosci Lett 151:229–233. CrossRef Medline

Mason AJ, Hayflick JS, Zoeller RT, Young WS 3rd, Phillips HS, Nikolics K, Seeburg PH (1986) A deletion truncating the gonadotropin-releasing hormone gene is responsible for hypogonadism in the hpg mouse. Science 234:1366–1371. CrossRef Medline

Mellon PL, Windle JJ, Goldsmith PC, Padula CA, Roberts JL, Weiner RI (1990) Immortalization of hypothalamic GnRH neurons by genetically targeted tumorigenesis. Neuron 5:1–10. CrossRef Medline

Nelson SB, Lawson MA, Kelley CG, Mellon PL (2000) Neuron-specific expression of the rat gonadotropin-releasing hormone gene is conferred by interactions of a defined promoter element with the enhancer in GT1-7 cells. Mol Endocrinol 14:1509–1522. CrossRef Medline

Novaira HJ, Fadoju D, Diaczok D, Radovick S (2012) Genetic mechanisms mediating kisspeptin regulation of GnRH gene expression. J Neurosci 32:17391–17400. CrossRef Medline

Novaira HJ, Sonko ML, Radovick S (2015) Kisspeptin induces dynamic chromatin modifications to control GnRH gene expression. Mol Neurobiol. Advance online publication. Retrieved Nov. 15, 2015. CrossRef Medline

Pielecka-Fortuna J, Chu Z, Moenter SM (2008) Kisspeptin acts directly and indirectly to increase gonadotropin-releasing hormone neuron activity and its effects are modulated by estradiol. Endocrinology 149:1979–1986. CrossRef Medline

Pitteloud N, Acierno JS Jr, Meysing A, Eliseenkova AV, Ma J, Ibrahimi OA, Metzger DL, Hayes FJ, Dwyer AA, Hughes VA, Yialamas M, Hall JE, Grant E, Mohammadi M, Crowley WF Jr (2006) Mutations in fibroblast growth factor receptor 1 cause both Kallmann syndrome and normosmic idiopathic hypogonadotropic hypogonadism. Proc Natl Acad Sci U S A 103:6281–6286. CrossRef Medline

Pitteloud N, Quinton R, Pearce S, Raivio T, Acierno J, Dwyer A, Plummer L, Hughes V, Seminara S, Cheng YZ, Li WP, Maccoll G, Eliseenkova AV, Olsen SK, Ibrahimi OA, Hayes FJ, Boepple P, Hall JE, Bouloux P, Mohammadi M, et al. (2007a) Digenic mutations account for variable phenotypes in idiopathic hypogonadotropic hypogonadism. J Clin Invest 117:457–463. CrossRef Medline

Pitteloud N, Zhang C, Pignatelli D, Li JD, Raivio T, Cole LW, Plummer L, Jacobson-Dickman EE, Mellon PL, Zhou QY, Crowley WF Jr (2007b) Loss-of-function mutation in the prokineticin 2 gene causes Kallmann syndrome and normosmic idiopathic hypogonadotropic hypogonadism. Proc Natl Acad Sci U S A 104:17447–17452. CrossRef Medline

Radovick S, Wray S, Lee E, Nicols DK, Nakayama Y, Weintraub BD, Westphal H, Cutler GB Jr, Wondisford FE (1991) Migratory arrest of gonadotropin-releasing hormone neurons in transgenic mice. Proc Natl Acad Sci U S A 88:3402–3406. CrossRef Medline

Rave-Harel N, Miller NL, Givens ML, Mellon PL (2005) The Groucho-related gene family regulates the gonadotropin-releasing hormone gene through interaction with the homeodomain proteins MSX1 and OCT1. J Biol Chem 280:30975–30983. CrossRef Medline

Rodríguez CI, Buchholz F, Galloway J, Sequerra R, Kasper J, Ayala R, Stewart AF, Dymecki SM (2000) High-efficiency deleter mice show that FLPe is an alternative to Cre-loxP. Nat Genet 25:139–140. CrossRef Medline

Schinckel AP, Johnson RK, Kittok RJ (1984) Relationships among measures of testicular development and endocrine function in boars. J Anim Sci 58:1255–1261. Medline

Schwanzel-Fukuda M, Pfaff DW (1989) Origin of luteinizing hormone-releasing hormone neurons. Nature 338:161–164. CrossRef Medline

Schwarting GA, Wierman ME, Tobet SA (2007) Gonadotropin-releasing hormone neuronal migration. Semin Reprod Med 25:305–312. CrossRef Medline

Soriano P (1999) Generalized *lacZ* expression with the ROSA26 cre reporter strain. Nat Genet 21:70–71. CrossRef Medline

Srinivas S, Watanabe T, Lin CS, William CM, Tanabe Y, Jessell TM, Costantini F (2001) Cre reporter strains produced by targeted insertion of EYFP and ECFP into the ROSA26 locus. BMC Dev Biol 1:4. CrossRef Medline

Take-uchi M, Clarke JD, Wilson SW (2003) Hedgehog signalling maintains the optic stalk-retinal interface through the regulation of Vax gene activity. Development 130:955–968. CrossRef Medline

Tsai PS, Gill JC (2006) Mechanisms of disease: insights into X-linked and autosomal-dominant Kallmann syndrome. Nat Clin Pract Endocrinol Metab 2:160–171. CrossRef Medline

Valdes-Socin H, Rubio Almanza M, Tome Fernandez-Ladreda M, Debray FG, Bours V, Beckers A (2014) Reproduction, smell, and neurodevelopmental disorders: genetic defects in different hypogonadotropic hypogonadal syndromes. Front Endocrinol (Lausanne) 5:109. CrossRef

Whyte DB, Lawson MA, Belsham DD, Eraly SA, Bond CT, Adelman JP, Mellon PL (1995) A neuron-specific enhancer targets expression of the gonadotropin-releasing hormone gene to hypothalamic neurosecretory neurons. Mol Endocrinol 9:467–477. CrossRef Medline

Wierman ME, Kiseljak-Vassiliades K, Tobet S (2011) Gonadotropin-releasing hormone (GnRH) neuron migration: initiation, maintenance and cessation as critical steps to ensure normal reproductive function. Front Neuroendocrinol 32:43–52. CrossRef Medline

Williams NI, Berga SL, Cameron JL (2007) Synergism between psychosocial and metabolic stressors: impact on reproductive function in cynomolgus monkeys. Am J Physiol Endocrinol Metab 293:E270–276. CrossRef Medline

Wolfe A, Divall S, Singh SP, Nikrodhanond AA, Baria AT, Le WW, Hoffman GE, Radovick S (2008) Temporal and spatial regulation of CRE recombinase expression in gonadotrophin-releasing hormone neurones in the mouse. J Neuroendocrinol 20:909–916. CrossRef Medline

Yoon H, Enquist LW, Dulac C (2005) Olfactory inputs to hypothalamic neurons controlling reproduction and fertility. Cell 123:669–682. CrossRef Medline